Supernova Neutrinos
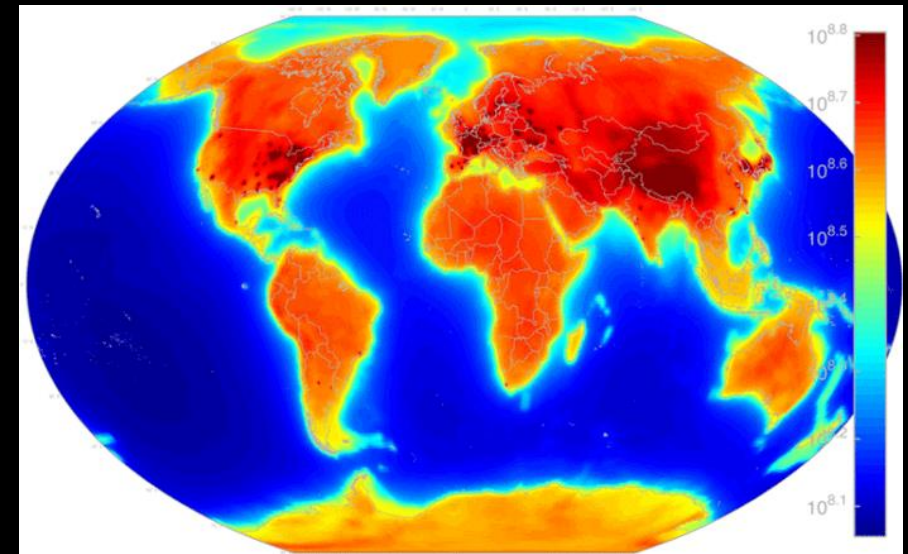
- Core collapse supernovae
- SN1987a neutrino signal
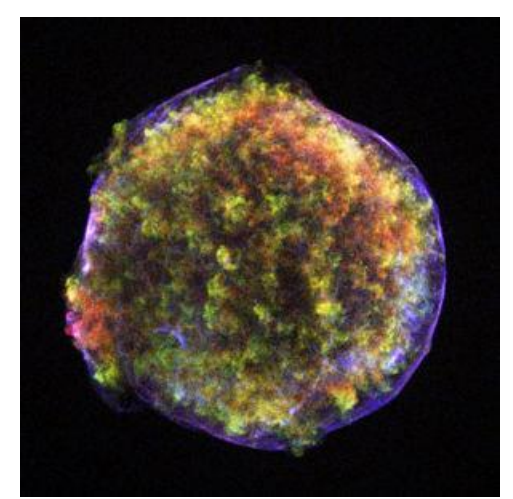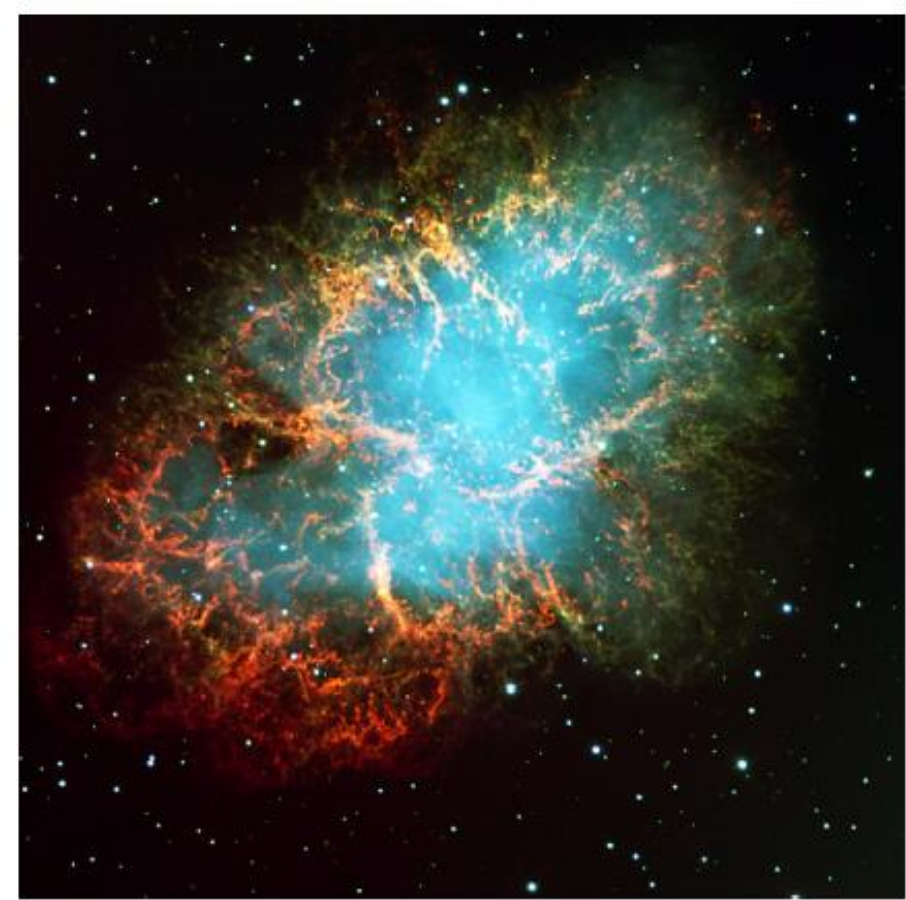- DSNB (diffuse supernova neutrino background

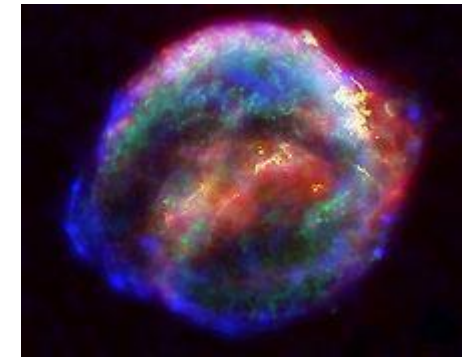Supernova explosions are the most energetic astrophysical events since the Big Bang

A star suddenly brightens
the peak of its lightcurve shines as bright as the host galaxy

Geo Neutrinos

SN1572 – discovered by Tycho Brahe
„NOVA" = „new Star"

SN1604 – Keplers Supernova

Fig. 32. – Remnant of the historical supernova of 1054. Left: Crab Nebula, the dispersed ejecta from the explosion. Credit: ESO (see also http://apod.nasa.gov/apod/ap991122.html). Right: Crab Pulsar in the center of the Crab Nebula, the compact neutron star remaining from the collapse, as a superposition of an HST optical image (red) and a false-color Chandra x-ray image (blue). Credit: J. Hester (ASU) et al., CXC, HST, NASA (see also http://apod.nasa.gov/apod/ap050326.html).

G.Raffelt:„Neutrinos and the Stars",arxiv: 1201.1637

The Death of Stars

TABLE III. – *Evolution of stars, depending on their initial mass.*

Mass Range	Evolution	End State
$M \lesssim 0.08\,M_\odot$	Hydrogen burning never ignites	Brown Dwarf
$0.08\,M_\odot \lesssim M \lesssim 0.8\,M_\odot$	Hydrogen burning not completed in Hubble time	Low-mass main-sequence star
$0.8\,M_\odot \lesssim M \lesssim 2\,M_\odot$	Degenerate helium core after hydrogen exhaustion	Carbon-oxygen white dwarf surrounded
$2\,M_\odot \lesssim M \lesssim 6\text{–}8\,M_\odot$	Helium ignition non-degenerate	by planetary nebula
$6\text{–}8\,M_\odot \lesssim M$	All burning phases → Onion skin structure → Core-collapse supernova	Neutron star (often pulsar) Sometimes black hole Supernova remnant (SNR) e.g. crab nebula

Neutrinos

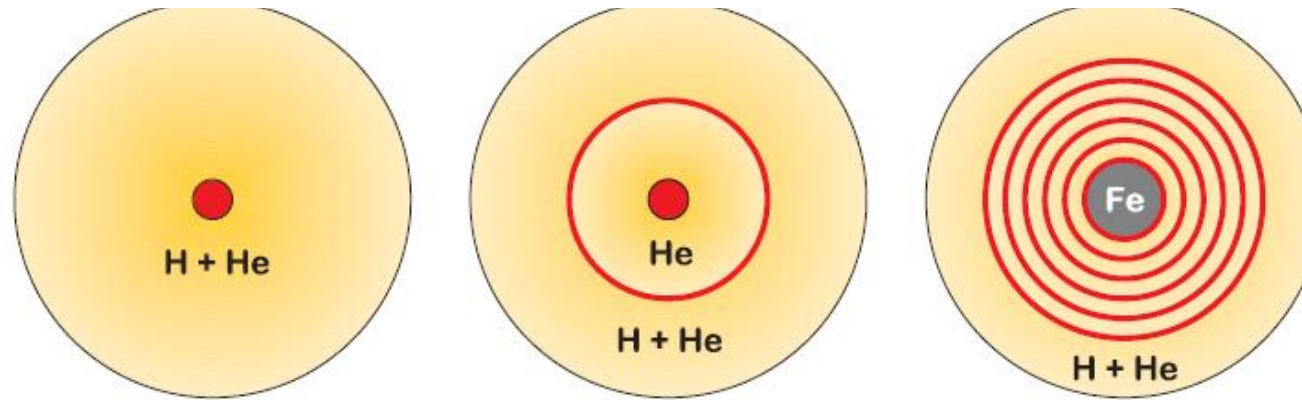

H + He   He   Fe
           H + He   H + He

Fig. 2. – Schematic structure of hydrogen and helium burning stars and final "onion skin structure" before core collapse.

Spectral Type Classification of Supernovae

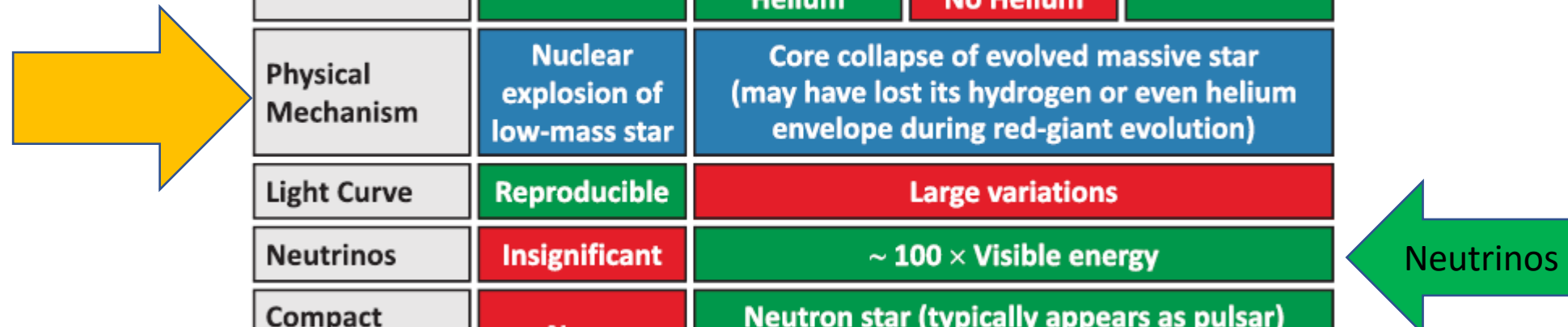| Spectral Type	Ia	Ib	Ic	II
Spectrum	Silicon	No Hydrogen		Hydrogen
		No Silicon		
		Helium	No Helium	
Physical Mechanism	Nuclear explosion of low-mass star	Core collapse of evolved massive star (may have lost its hydrogen or even helium envelope during red-giant evolution)		
Light Curve	Reproducible	Large variations		
Neutrinos	Insignificant	$\sim 100 \times$ Visible energy		
Compact Remnant	None	Neutron star (typically appears as pulsar) Sometimes black hole		
Rate / h^2 SNu	0.36 ± 0.11	0.14 ± 0.07		0.71 ± 0.34
Observed	Total ~ 5600 as of 2011 (Asiago SN Catalogue)			

Neutrinos

Fig. 33. – Spectral classification of supernovas. The rate is measured in the supernova unit, $1\ \mathrm{SNu} = 1$ SN per century per $10^{10}\ L_{\odot,B}$ (B-band solar luminosity).

Naming of supernovae: SN2011A is the first SN in the year 2011,...
until 2011Z then 2011aa, 2011ab, etc.

Core Collapse Supernovae
Basic Considerations

- Star with $M > 6-8 M_\odot$ nuclear fusion reactions until Fe core

- in the core no more pressure from nuclear energy release
  - ↳ pressure from degenerate core builds up (two fermions cannot sit at same location)
  - ↳ but core collapse starts when core reaches
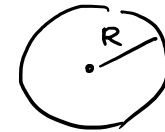
  Chandrasekar limit $M_{ch} = 1.457 M_\odot$ neutron star

$$\rho = \rho_{nuclear} = 2 \cdot 10^{14}\ \text{g}/\text{cm}^3$$
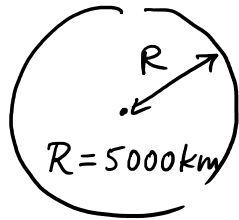
R = 5000 km
Fe core
$M = 1.5 M_\odot$

Collapse until

R = 12 km
$M \approx 1.5 M_\odot$

Gravitational binding energy $E_G = -\dfrac{3}{5}\dfrac{Gm^2}{r}$ (G is Newton constant)

Core collapse: $\Delta E_G = 3 \cdot 10^{53}\ erg = 3 \cdot 10^{46}\ J$

$\hat{=}\ 0.12 M_\odot$ (9% of M_{core})

$3 \cdot 10^{53}$ erg emitted in Core Collapse SN

- 99% in neutrinos!
- 1% in kinetic energy
- 0.01% in optical outburst (which is brighter than host galaxy)

Neutrinos of all flavors $(\nu, \bar{\nu})$ are emitted over few seconds

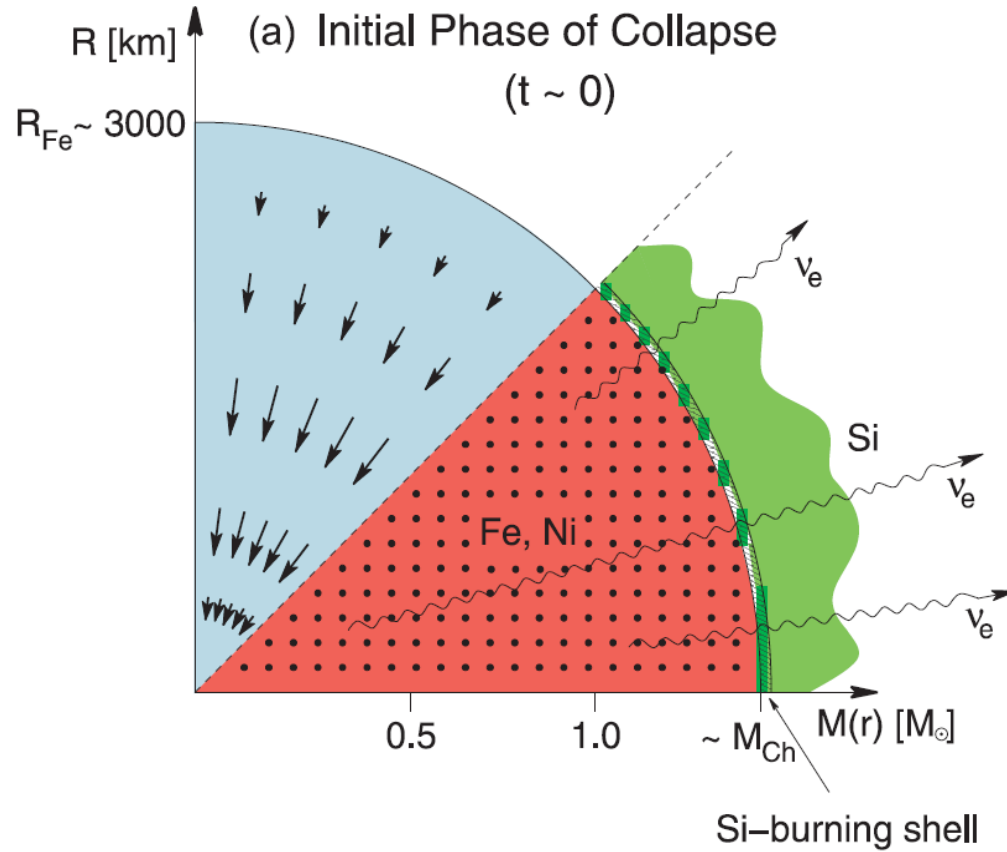$\langle E_\nu \rangle \approx 15$ MeV (depending a little bit on flavor)

$$N_\nu = \frac{0.99 \cdot \Delta E_G}{\langle E_\nu \rangle} = \frac{0.99 \cdot 3 \cdot 10^{46} J}{15 \cdot 10^6 \cdot 1.6 \cdot 10^{-19} J} \approx 10^{58}$$

SN at distance $\underbrace{10 \text{ kpc}}_{3 \cdot 10^4 \text{ Lyrs}}$ (distance Earth – center of Milky Way 8kpc)

$$F_\nu = \frac{N_\nu}{4 \pi d^2} \approx 10^{12} \frac{\nu}{cm^2} \quad \text{„Fluence" within few seconds}$$

Stages of Core Collapse Supernovae

(a) **Initial phase of collapse.** A Chandrasekhar-mass iron-nickel core of an evolved massive star becomes unstable. Electrons squeezed into high-energy states begin to dissociate the heavy nuclei, convert to neutrinos, escape, and in this way accelerate the loss of pressure. Photo dissociation of heavy nuclei is also important.
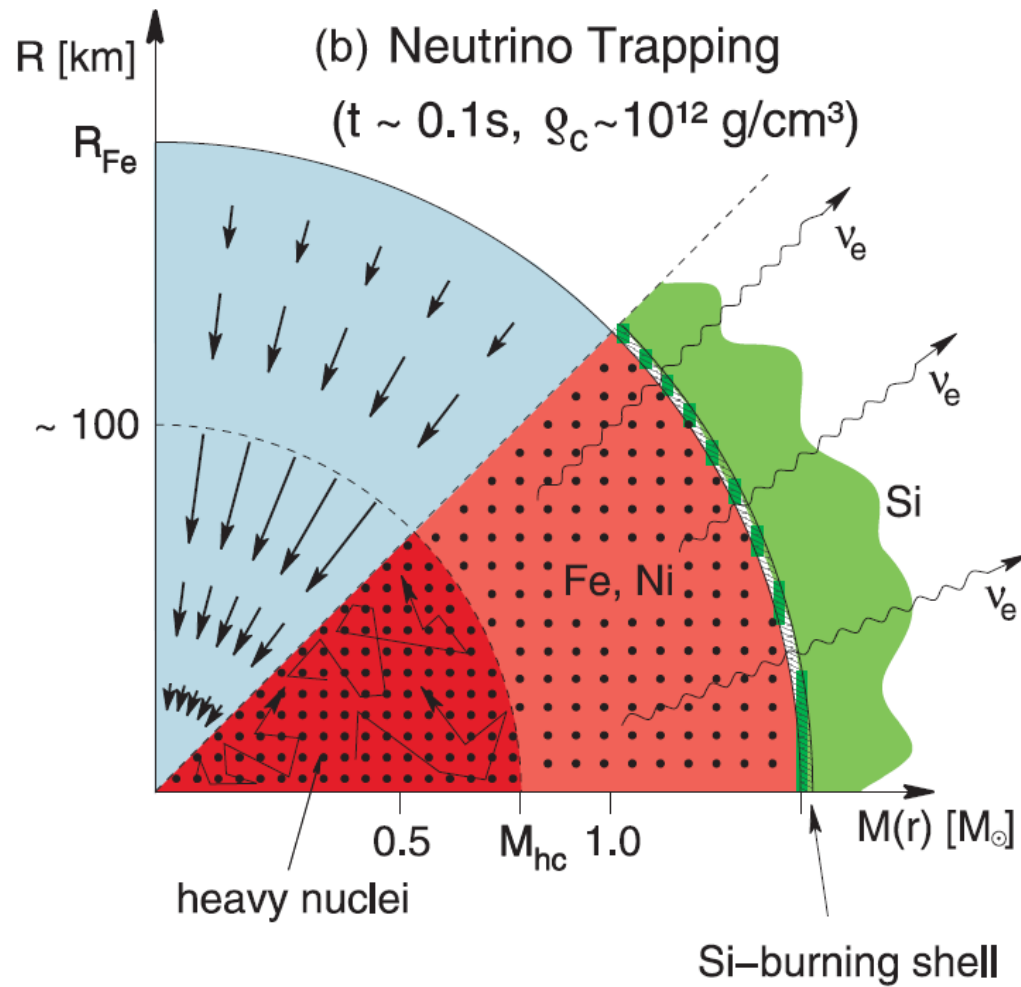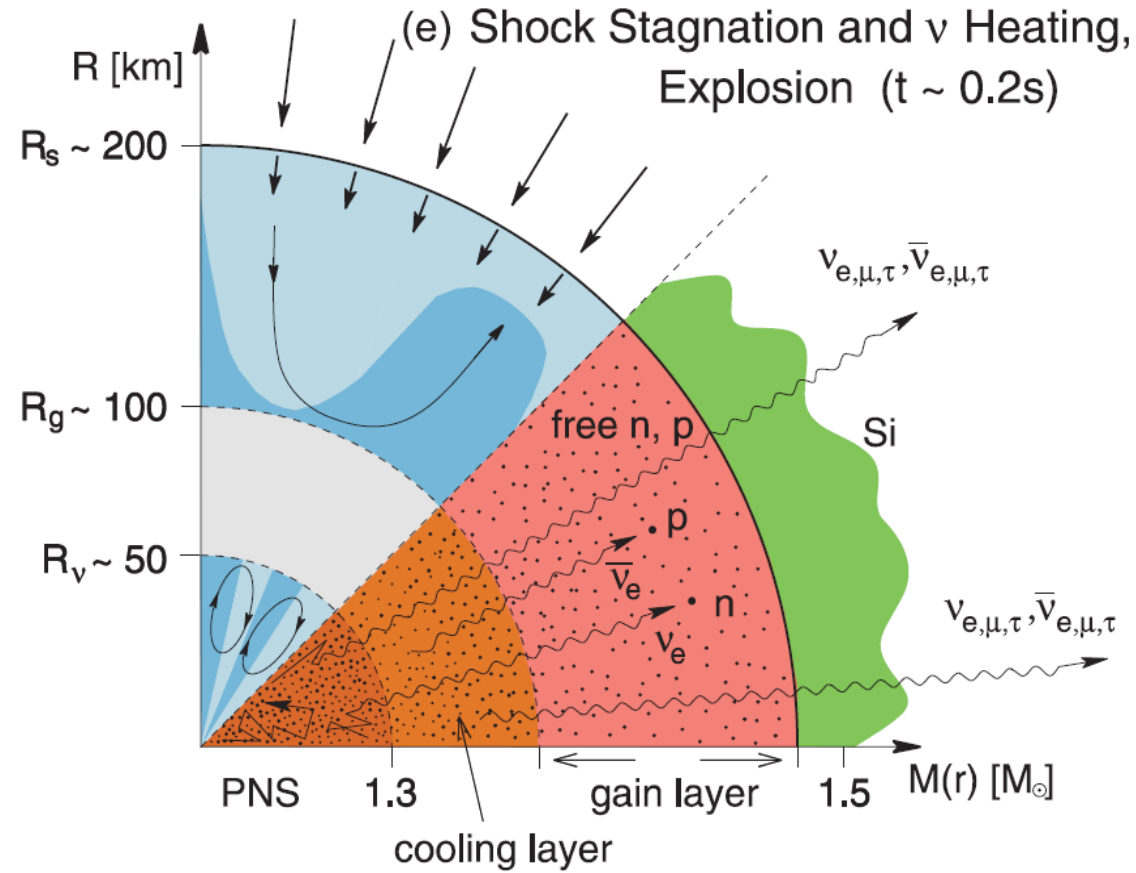
(b) **Neutrino trapping.** The core collapses, separated into a nearly homologous inner core that remains in hydrodynamic contact with itself, and the outer core with supersonic collapse. When densities of about 10^{12} g cm^{-3} are reached, neutrinos are trapped by coherently enhanced elastic scattering on large nuclei.
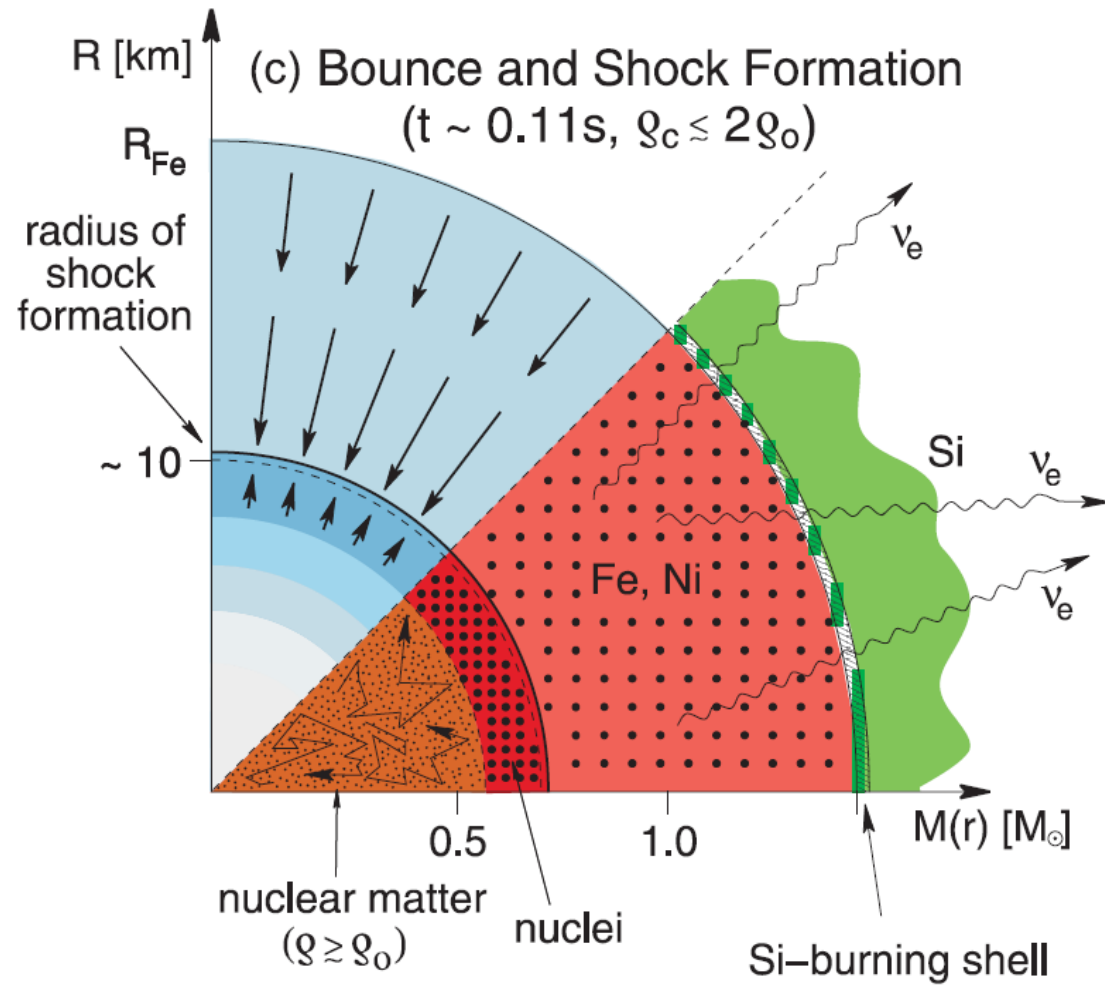
(c) **Bounce and shock formation.** The inner core reaches nuclear density of about 3×10^{14} g cm^{-3}, the EoS stiffens, the collapse halts, and the supersonic infall rams into a "solid wall" and gets reflected, forming a shock wave. Across the outward moving shock wave, the velocity field jumps discontinuously from supersonic inward to outward motion. The density also jumps discontinuously across the shock wave.
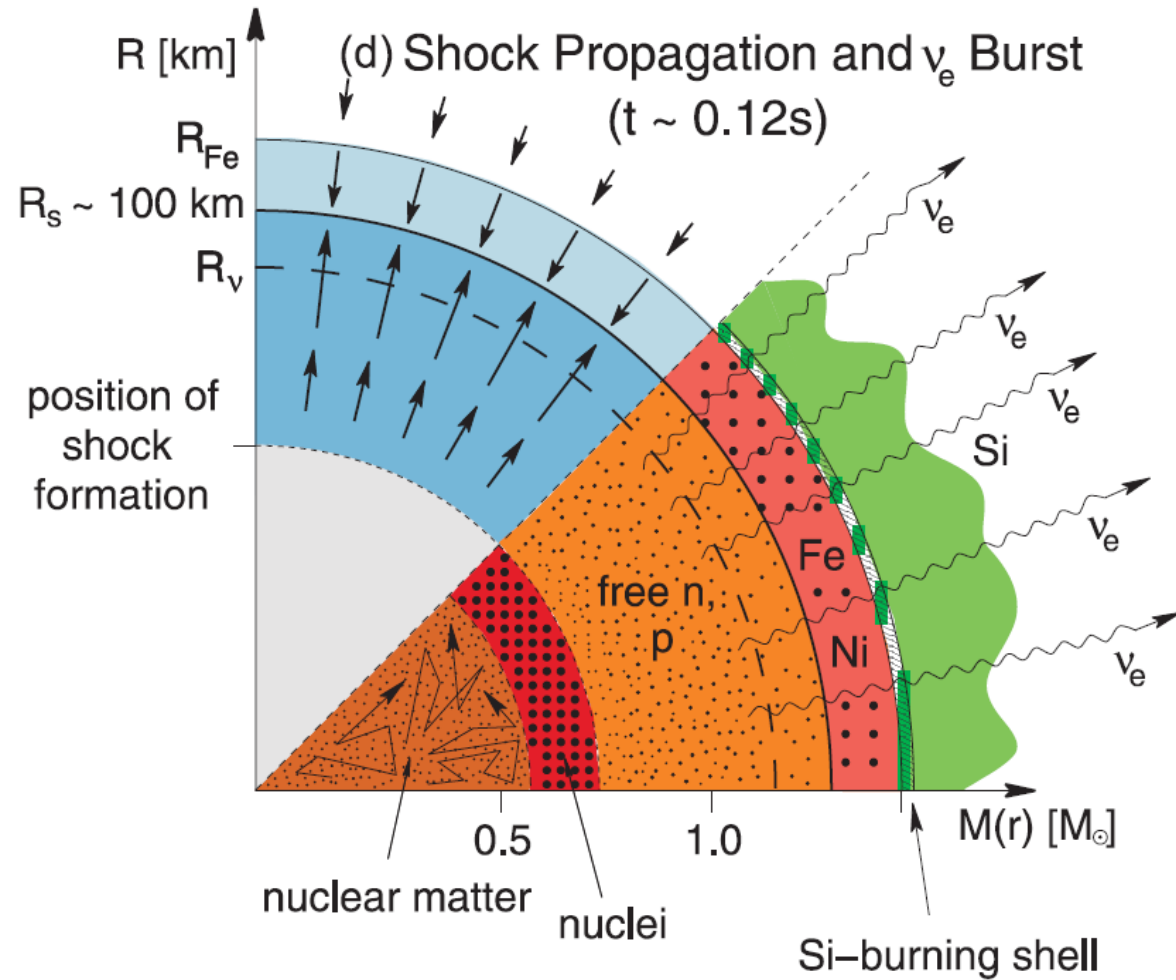
(d) **Shock propagation and ν_e burst.** The shock propagates outward and eventually reaches the edge of the iron core. The dissociation of this layer allows for electron capture, $e^- + p \rightarrow n + \nu_e$, producing the "prompt ν_e burst" or "prompt deleptonization burst." Only the outer $\sim 0.1\,M_\odot$ of the former iron core deleptonizes in this way, deeper layers deleptonize slowly on the diffusion time scale of seconds.

(e) Shock Stagnation and ν Heating, Explosion (t ~ 0.2s)

Figure labels: R [km]; $R_s \sim 200$; $R_g \sim 100$; $R_\nu \sim 50$; free n, p; Si; $\nu_{e,\mu,\tau}, \bar{\nu}_{e,\mu,\tau}$; $\bar{\nu}_e$; p; n; ν_e; PNS; 1.3; cooling layer; gain layer; 1.5; $M(r)$ [$M_\odot$]

(e) **Shock stagnation, neutrino heating, explosion.** The shock wave runs out of pressure and stagnates at a radius of 150–200 km. Matter keeps falling in ("accretion shock"), i.e. the shock wave surfs on the infalling material that deposits energy near the nascent neutron star and powers a strong neutrino luminosity that is dominated by $\nu_e\bar{\nu}_e$ pairs. Convection sets in. Neutrino streaming continues to heat the material behind the shock wave, building up renewed pressure. After several hundred ms the shock wave takes off, expelling the overlying material.
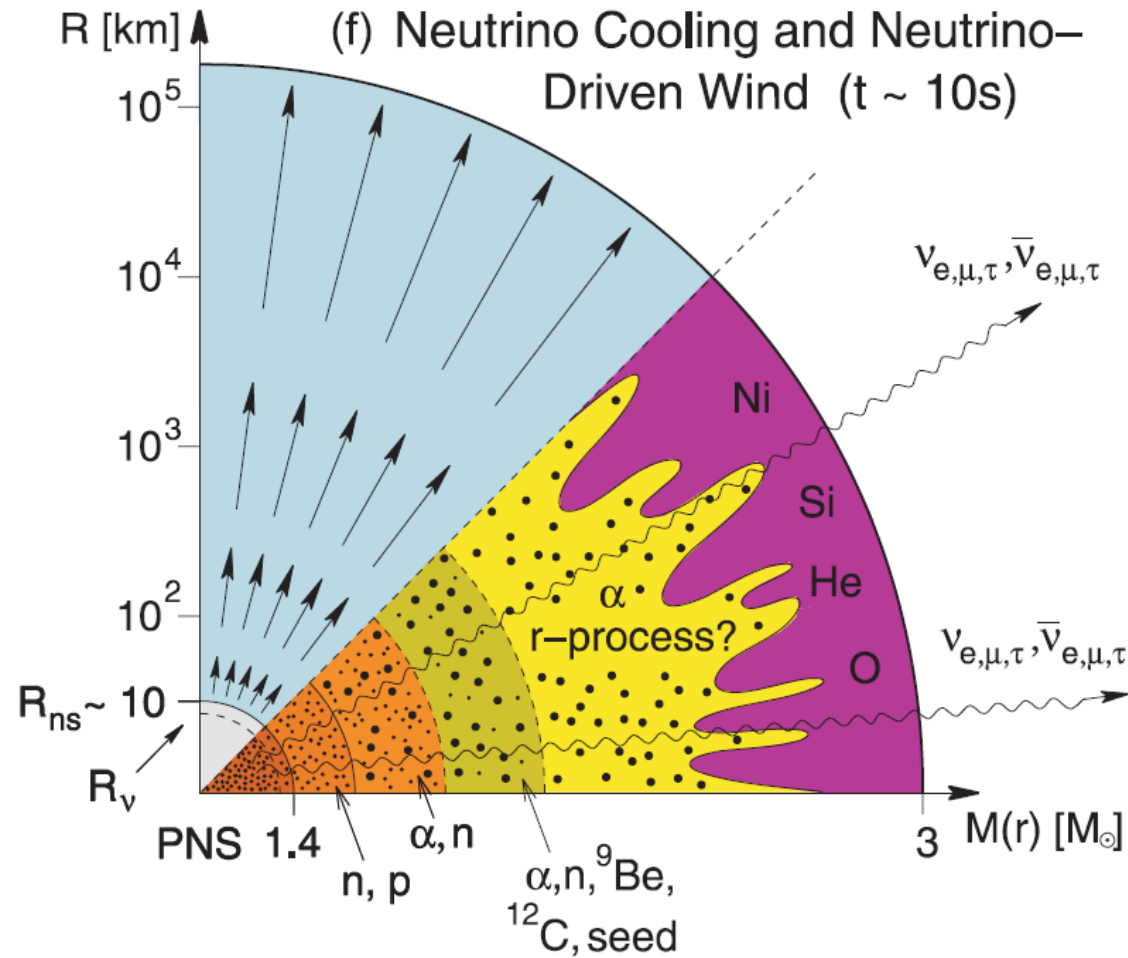
(f) **Neutrino cooling and neutrino-driven wind.** The neutron star settles to about 12 km radius and cools by diffusive neutrino emission over seconds. A wind of matter is blown off with chemical composition governed by neutrino processes. Nucleosynthesis takes place in this "hot bubble" region, conceivably including the r-process production of heavy neutron-rich elements.
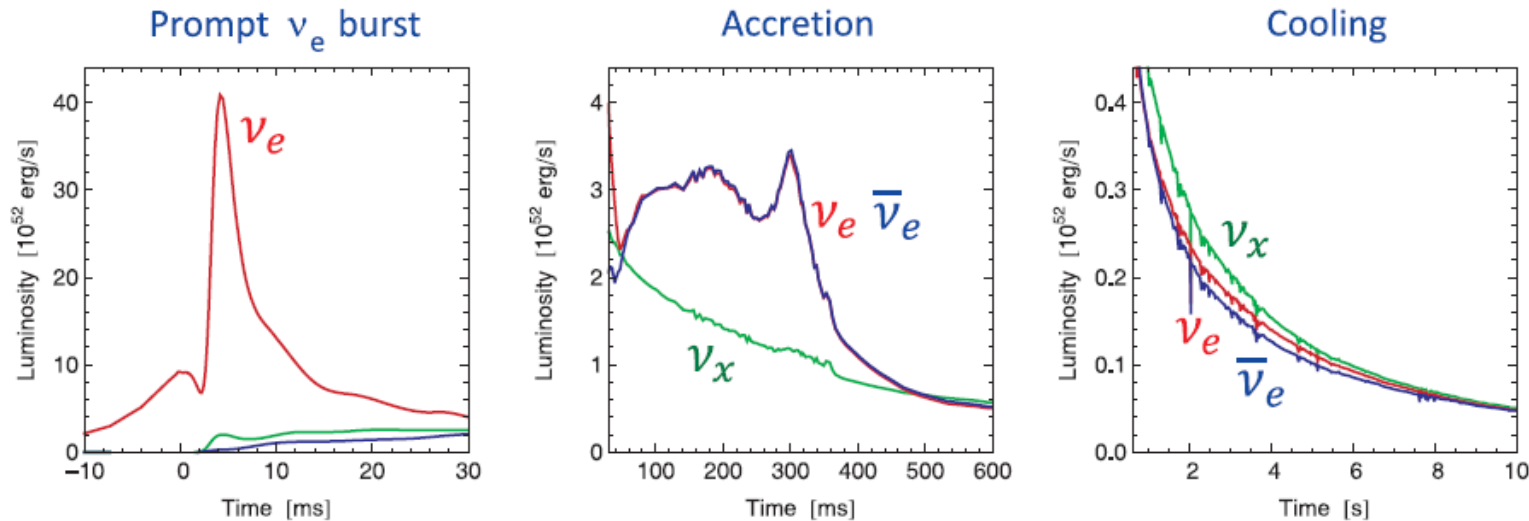
Fig. 39. – Neutrino signal using data from a spherically symmetric $10.8\,M_\odot$ simulation of the Basel group [141]. The explosion was manually triggered.

(1) **Prompt ν_e burst.** The shock wave breaks through the edge of the core, allowing for fast electron capture on free protons. A ν_e burst (5–10 ms) from deleptonization of the outer core layer emerges, the emission of $\bar\nu_e$ and ν_x is slowly beginning. This phase should not depend much on the progenitor mass.

(2) **Accretion phase.** The shock wave stagnates and matter falls in, releasing gravitational energy that powers neutrino emission. The ν_e and $\bar\nu_e$ luminosities are similar, but the ν_e number flux is larger, carrying away the lepton number of the infalling material. The heavy-lepton flavors are emitted closer to the SN core, and their flux is smaller, but their energies larger. So we typically have a hierarchy $L_{\nu_e} \sim L_{\bar\nu_e} > L_{\nu_x}$ and $\langle E_{\nu_e}\rangle < \langle E_{\bar\nu_e}\rangle < \langle E_{\nu_x}\rangle$, with $\langle E_{\bar\nu_e}\rangle \sim 12$–13 MeV. The duration of the accretion phase, typically a few hundred ms, and the detailed neutrino signal depend on the mass profile of the accreted matter.

(3) **Cooling phase.** The shock wave takes off, accretion stops, the SN core settles to become a neutron star, and cools by neutrino emission. The energy stored deep in its interior, largely in the form of e and ν_e degeneracy energy, emerges on a diffusion time scale of seconds. The luminosities of all species are similar $L_{\nu_e} \sim L_{\bar\nu_e} \sim L_{\nu_x}$ and decrease roughly exponentially with time. The ν_e number flux is larger because of deleptonization. The average energies follow the hierarchy $\langle E_{\nu_e}\rangle < \langle E_{\bar\nu_e}\rangle \sim \langle E_{\nu_x}\rangle$ and decrease with time. The characteristics of the cooling phase probably do not depend strongly on the progenitor mass.

Energy spectrum of SN Neutrinos
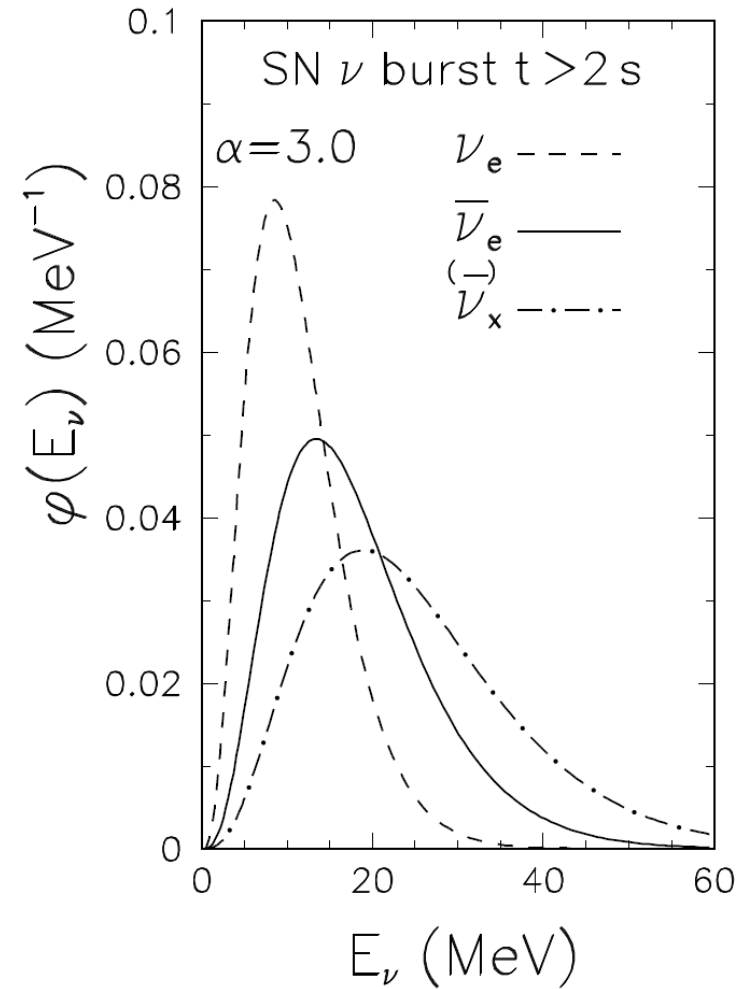
Fogli et al. hep-ph/0412046v2

Supernova SN1987A

Neutrino detectors taking data in 1987

Scintillator Detectors:
- **BST:** Baksan Scintillator Telescope (Russia), since 1980, M = 200t
- **LSD:** Liquid Scintillator Detector (Mont Blanc Tunnel), since 1984, M = 90t

Water Cherenkov Detectors:
- **IMB:** Irvine-Michigan-Brookhaven Detector (US), since 1982, M = 6800t
- **Kamiokande** (Japan), since 1983, M = 2140t
  had been just upgraded to Kamiokande-II and started in January 1987

can detect $\overline{\nu}_e$ in inverse beta decay reaction

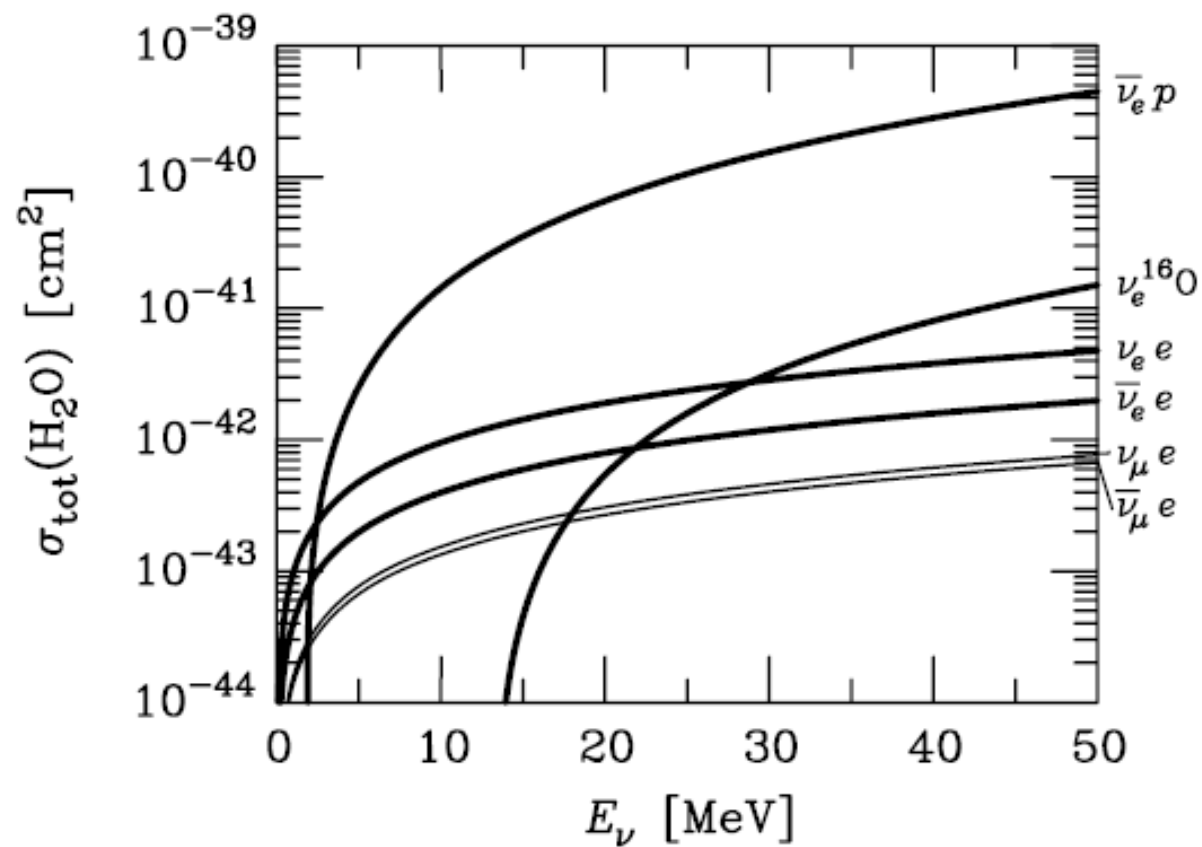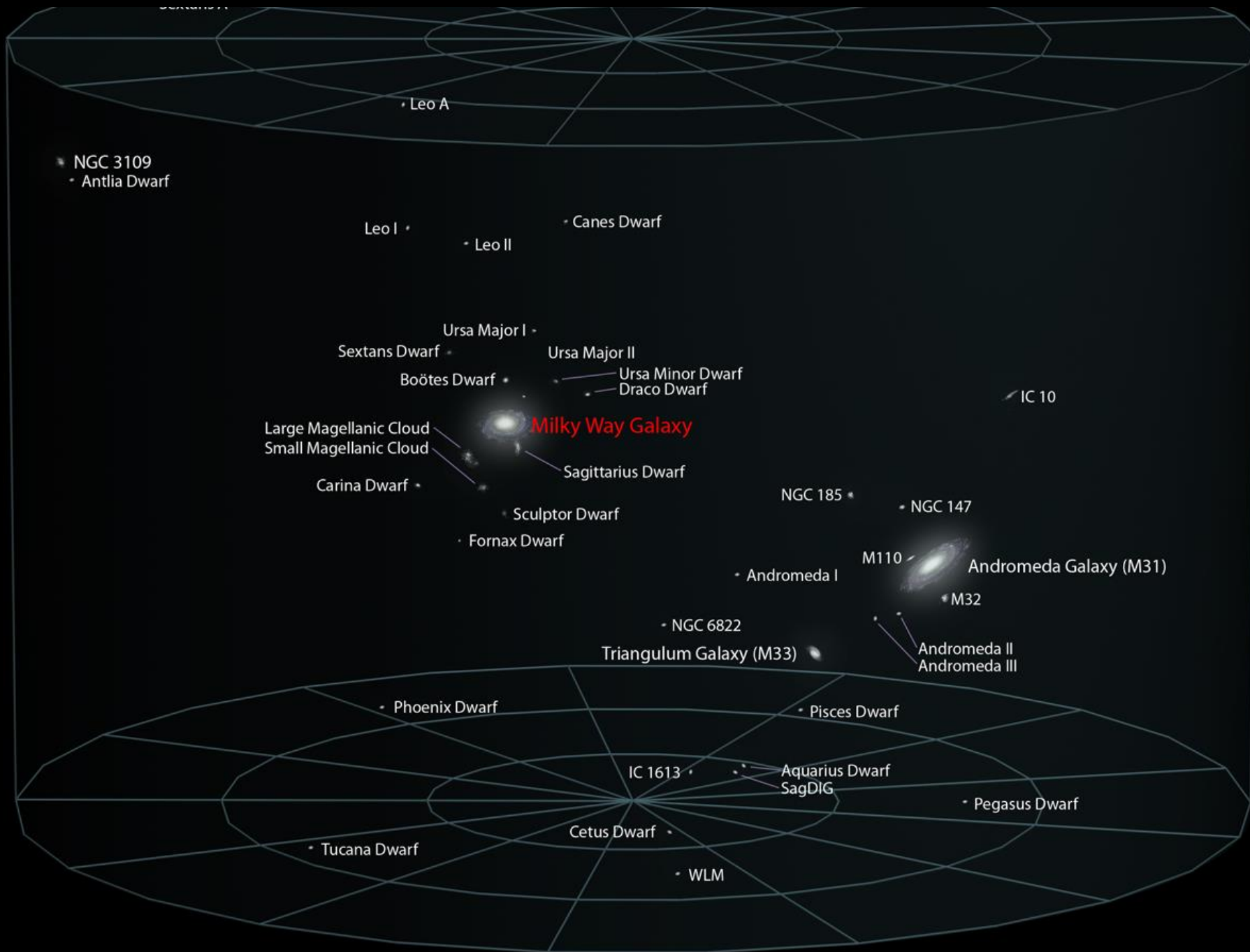$$\overline{\nu}_e + p \rightarrow e^+ + n$$

Fig. 45. – Total cross section per water molecule for the measurement of neutrinos in a water Cherenkov detector. A factor of 2 for protons and 10 for electrons is already included. A SN neutrino signal is primarily detected by inverse beta decay $\bar{\nu}_e + p \rightarrow n + e^+$.
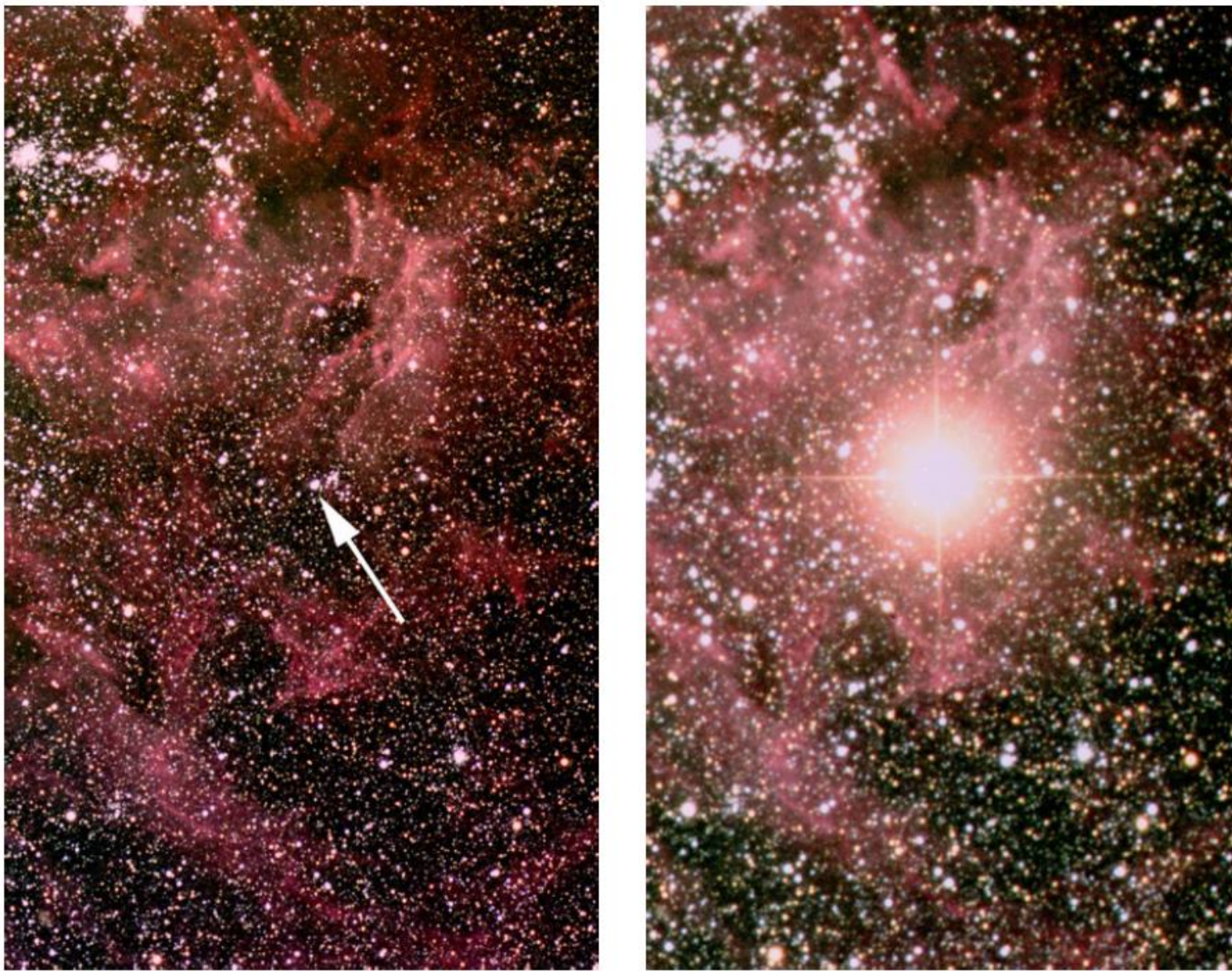
Fig. 31. – The blue supergiant star Sanduleak −69 202 in the Large Magellanic Cloud, before and after it exploded on 23 February 1987 (SN 1987A). This was the closest observed SN since Kepler's SN of 1603 and was the first example of a SN where the progenitor star could be identified. © Australian Astronomical Observatory.
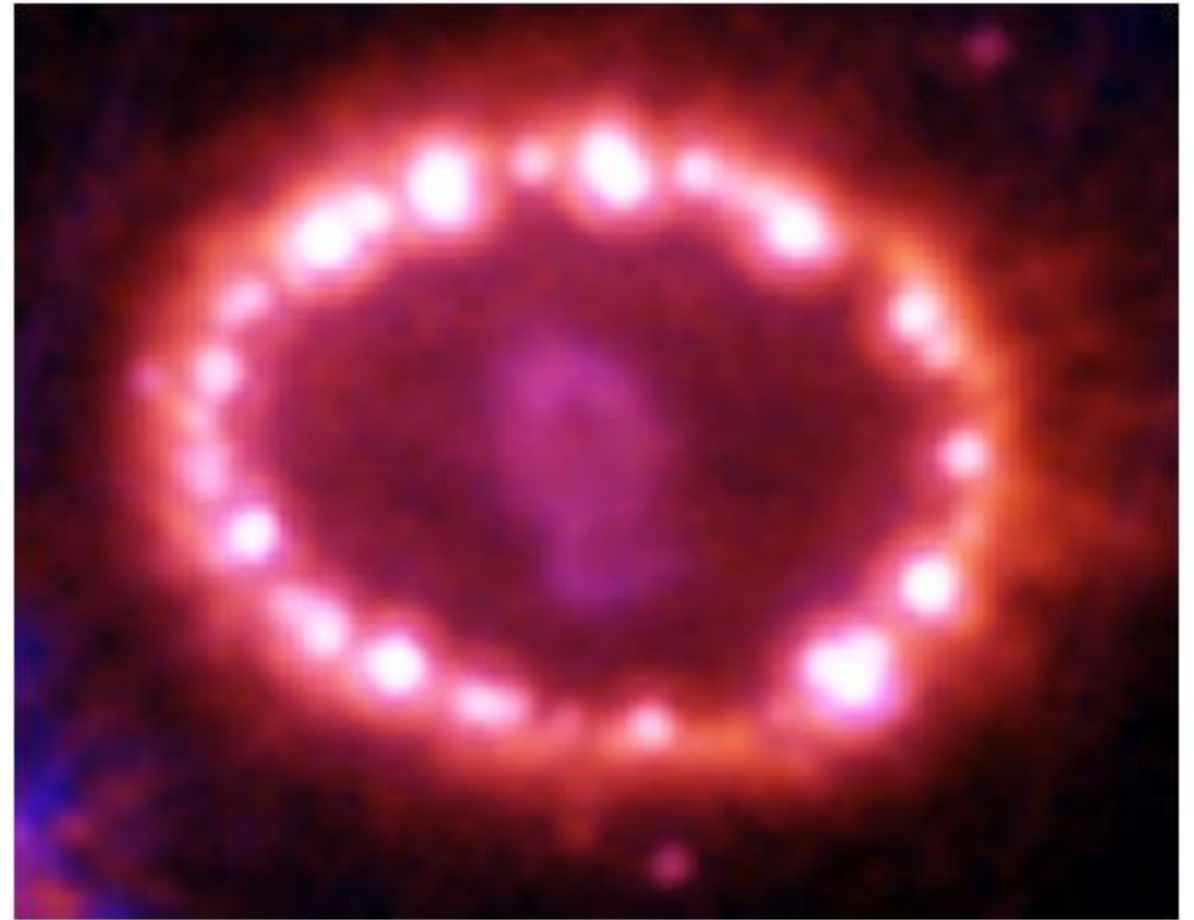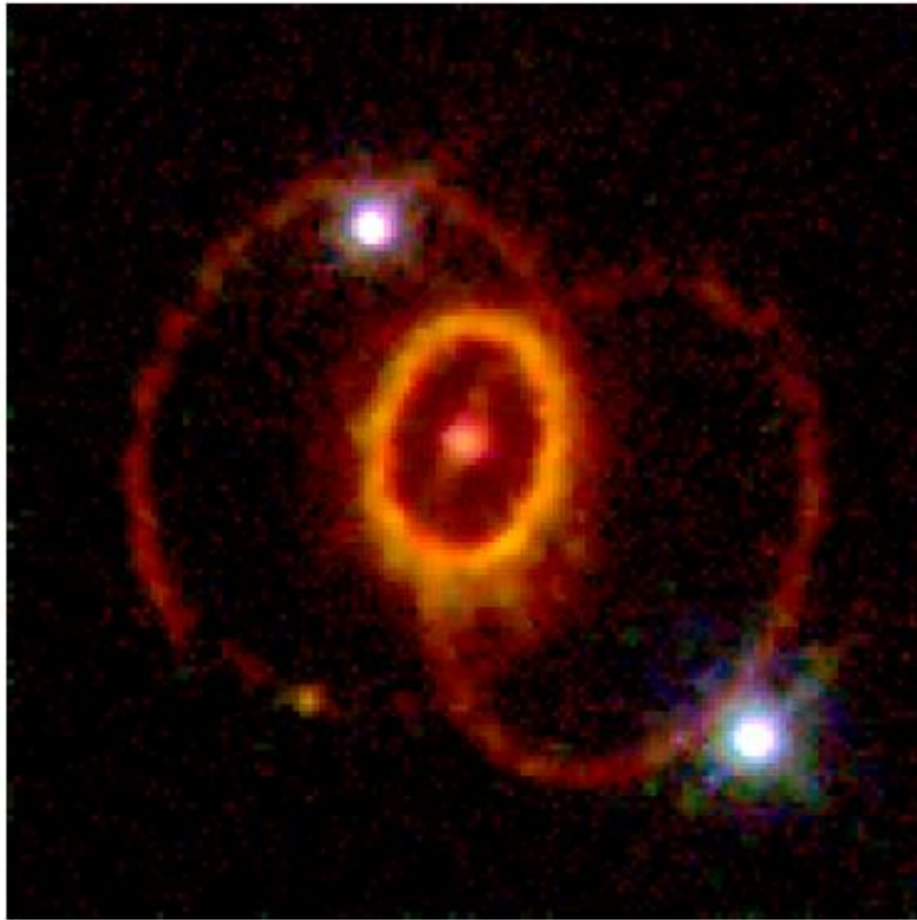
Fig. 43. – Rings of SN 1987A illuminated by the explosion. Left: Hubble Space Telescope image, taken in Feb. 1994. Credit: C. Burrows, ESA/STScI and NASA. Right: Image of inner ring, taken 28 Nov. 2003, showing bright spots caused by the supernova shock wave hitting the gas. The elongated "nebula" inside the ring is the supernova remnant. Credit: NASA, P. Challis, R. Kirshner (Harvard-Smithsonian Center for Astrophysics) and B. Sugerman (STScI).
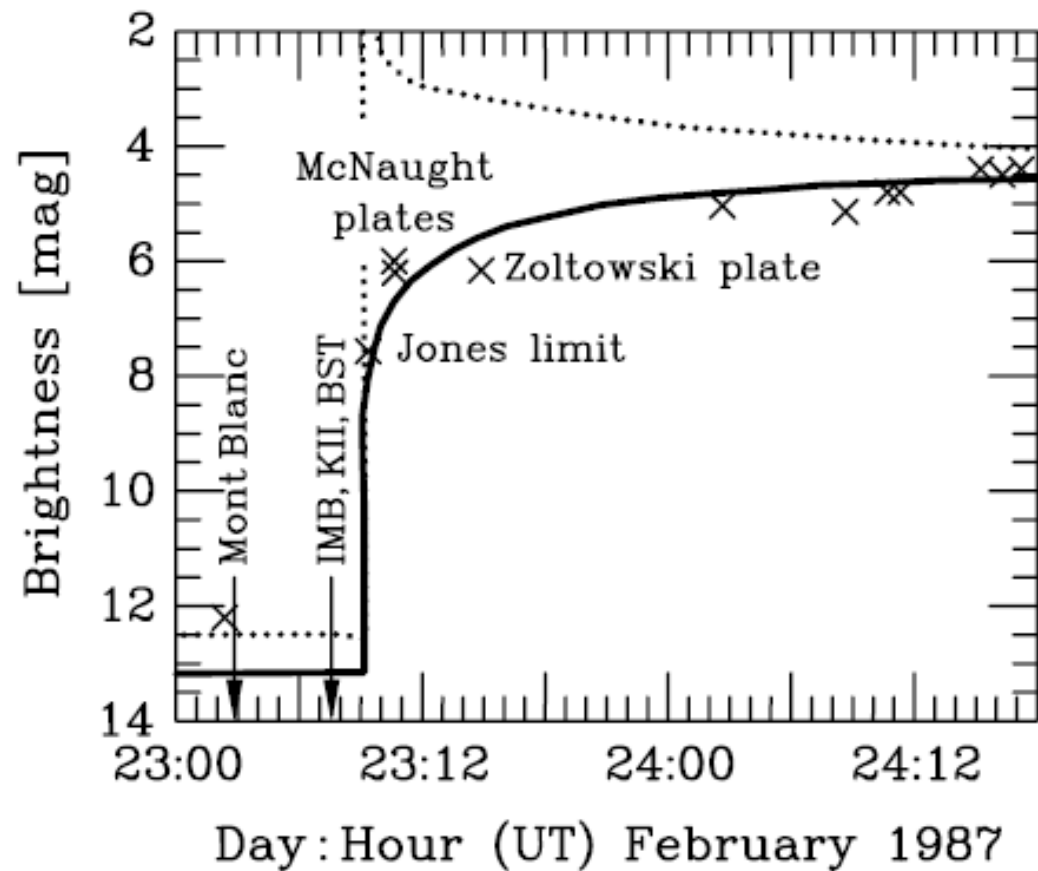
Fig. 46. – Early optical observations of SN 1987A according to the IAU Circulars, notably No. 4316 of February 24, 1987. The times of the IMB, Kamiokande II (KII) and Baksan (BST) neutrino observations (23:07:35) and of the Mont Blanc events (23:02:53) are also indicated. The solid line is the expected visual brightness, the dotted line the bolometric brightness according to model calculations. (Adapted, with permission, from Arnett et al. 1989 [166], Annual Review of Astronomy and Astrophysics, Volume 27, © 1989, by Annual Reviews Inc.)
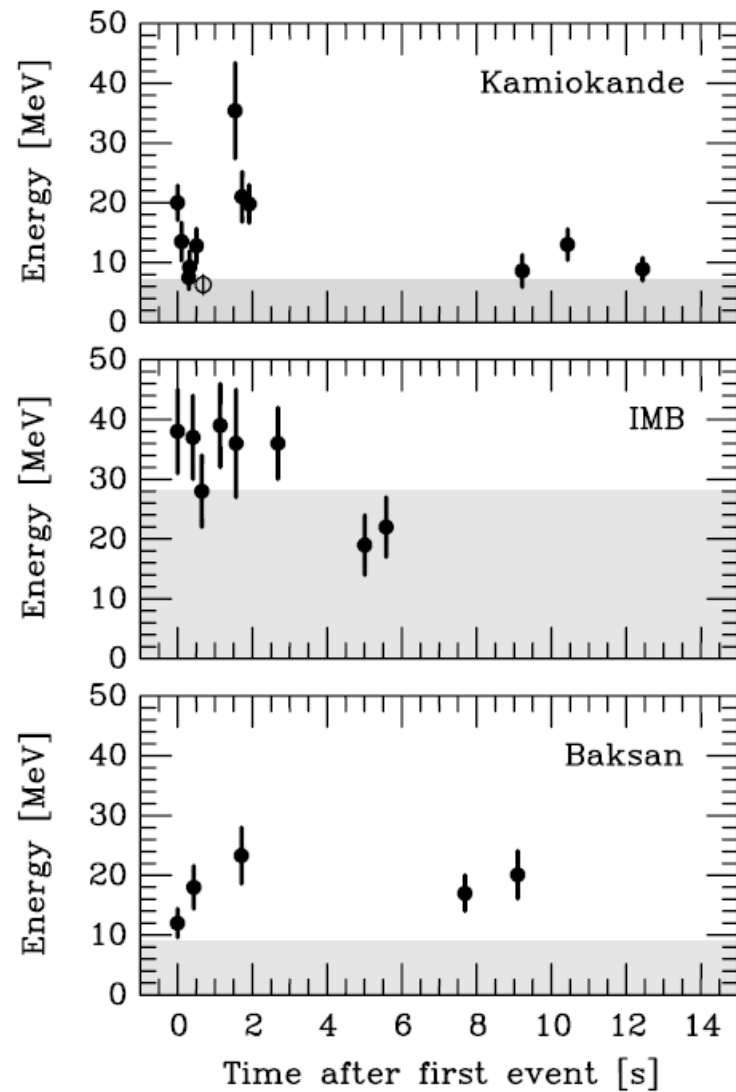
Fig. 47. – SN 1987A neutrino observations at Kamiokande [155, 156], IMB [157, 158] and Baksan [159, 160]. The energies refer to the secondary positrons from $\bar{\nu}_e p \rightarrow n e^+$. In the shaded area the trigger efficiency is less than 30%. The clock uncertainties are reported to be ± 1 min in Kamiokande, ± 50 ms in IMB, and $+2/-54$ s in BST; in each case the first event was shifted to $t = 0$. In Kamiokande, the event marked as an open circle is attributed to background.

TABLE IX. – *Existing and near-future SN neutrino detectors and event rates for a SN at 10 kpc, emission of 5×10^{52} erg in $\bar{\nu}_e$, average energy 12 MeV, and thermal energy distribution. For HALO and ICARUS, the event rates depend on assumptions about the other species. For references and details see Ref. [173] .*

Detector	Type	Location	Mass [kt]	Events	Status
IceCube	Ice Cherenkov	South Pole	0.6/OM	10^6	Running
Super-K IV	Water	Japan	32	7000	Running
LVD	Scintillator	Italy	1	300	Running
KamLAND	Scintillator	Japan	1	300	Running
SNO+	Scintillator	Canada	1	300	Commissioning 2013
MiniBOONE	Scintillator	USA	0.7	200	Running
Borexino	Scintillator	Italy	0.3	80	Running
BST	Scintillator	Russia	0.2	50	Running
HALO	Lead	Canada	0.079	tens	Almost ready
ICARUS	Liquid argon	Italy	0.6	200	Running

Expected #events for JUNO (SN @ 10kpc)

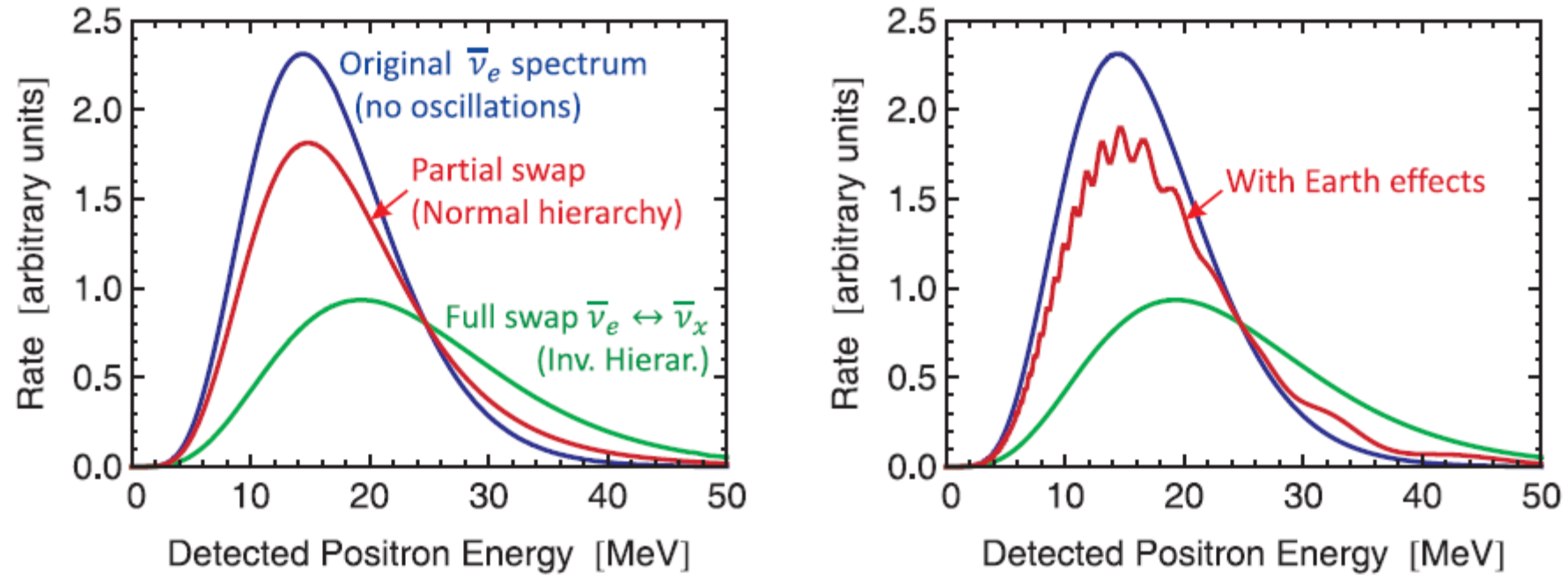| Channel	Type	Events for different $\langle E_\nu \rangle$ values		
		12 MeV	14 MeV	16 MeV
$\bar{\nu}_e + p \rightarrow e^+ + n$	CC	4.3×10^3	5.0×10^3	5.7×10^3
$\nu + p \rightarrow \nu + p$	NC	0.6×10^3	1.2×10^3	2.0×10^3
$\nu + e \rightarrow \nu + e$	ES	3.6×10^2	3.6×10^2	3.6×10^2
$\nu + {}^{12}C \rightarrow \nu + {}^{12}C^*$	NC	1.7×10^2	3.2×10^2	5.2×10^2
$\nu_e + {}^{12}C \rightarrow e^- + {}^{12}N$	CC	0.5×10^2	0.9×10^2	1.6×10^2
$\bar{\nu}_e + {}^{12}C \rightarrow e^+ + {}^{12}B$	CC	0.6×10^2	1.1×10^2	1.6×10^2

Fig. 61. – Accretion-phase $\bar{\nu}_e$ signal in water Cherenkov or scintillator detectors for different oscillation scenarios. For the regeneration effect (right panel) an 8000 km path length in the Earth is assumed.

TABLE X. – *Estimated rate of galactic core-collapse SNe per century.*

Method	Rate	Authors	Refs.
Scaling from external galaxies	2.5 ± 0.9	van den Bergh & McClure (1994)	[197, 199]
	1.8 ± 1.2	Cappellaro & Turatto (2000)	[198, 111]
Gamma-rays from galactic ^{26}Al	1.9 ± 1.1	Diehl et al. (2006)	[199]
Historical galactic SNe (all types)	5.7 ± 1.7	Strom (1994)	[200]
	3.9 ± 1.7	Tammann et al. (1994)	[201]
No neutrino burst in 30 years[a]	< 7.7 (90% CL)	Alekseev & Alekseeva (2002)	[202]

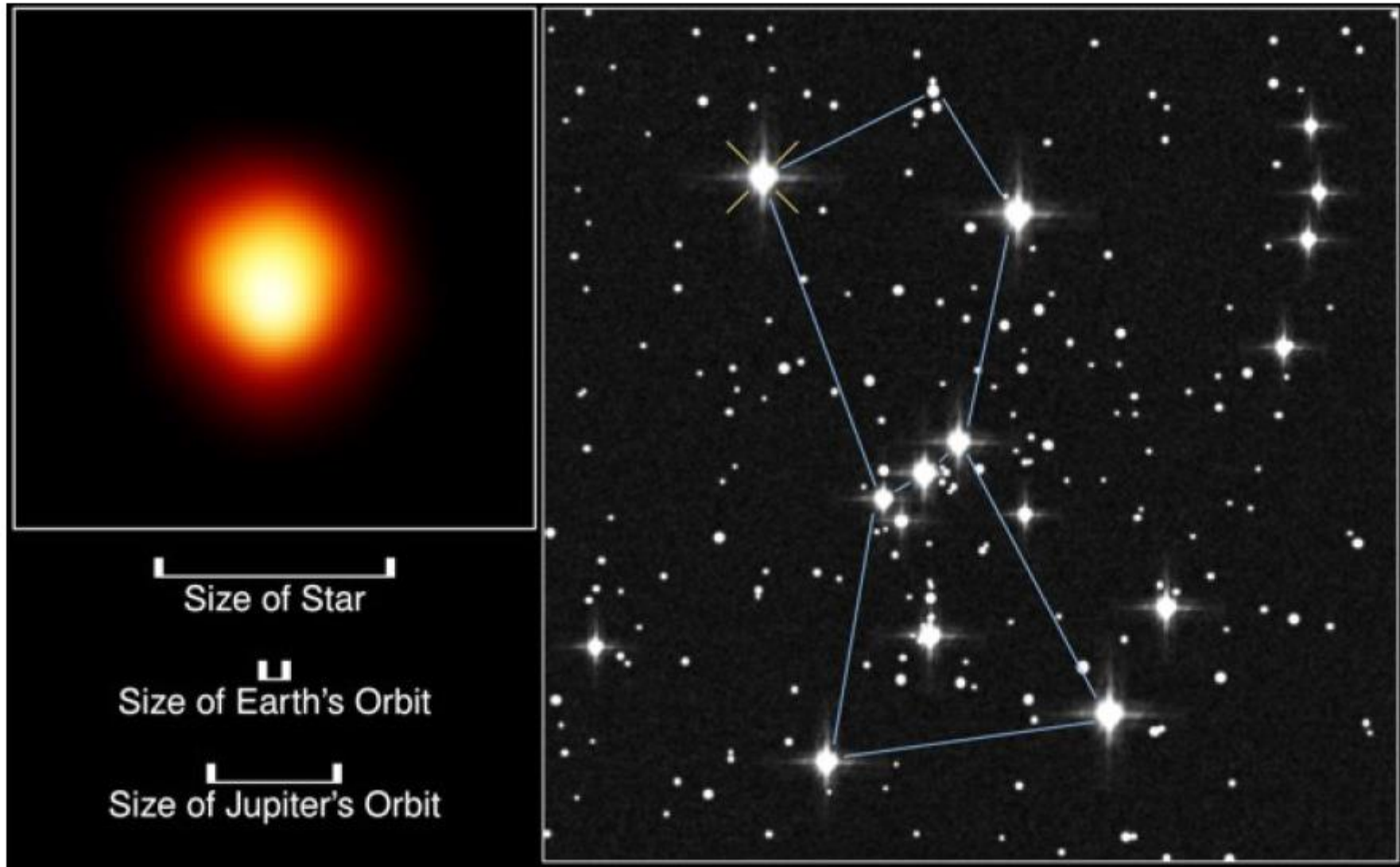[a]We have scaled the limit of Ref. [202] to 30 years of neutrino sky coverage.

Fig. 54. – The star Betelgeuze (Alpha Orionis) at a distance of 130 pc (425 lyr) is the first resolved image of a star other than the Sun. It is a candidate for the next nearby SN explosion. HST image taken in ultraviolet on 3 March 1995. Credit: A. Dupree (Harvard-Smithsonian CfA), R. Gilliland (STScI), NASA and ESA.

SCIENTIFIC AMERICAN

Betelgeuse's Brightening Raises Hopes for a Supernova Spectacle

Betelgeuse, the red star at the shoulder of the constellation Orion, has been acting strange, raising hopes for the spectacle of a lifetime

By Meghan Bartels on May 15, 2023

Subscribe

BBC Sky at Night MAGAZINE

Is Earth in danger if Betelgeuse goes supernova?

Red giant star Betelgeuse, could go supernova relatively soon. Are we in danger? Patrick Moore weighs up the risk in this archive article.

Diffuse Supernova Neutrino Background

(Supernova Relic Neutrinos SRN)

Neutrinos produced in SN outburst, that have diffused in universe

- 10^{18} SN so far in this universe
- a few SN explosions every second

~~Fluence~~ Flux of SNR:

$$\frac{dF_\nu}{dE_\nu} = C \int_0^{z_{max}} R_{SN}(z) \; \frac{dN_\nu(E'_\nu)}{dE'_\nu} (1+z) \frac{dt}{dz} dz$$

Redshift

SN-Rate

SN ν energy spectrum

Interesting
Contribution of "failed" SN

Super-Kamiokande Gadolinium Project (SK-Gd)

- Dissolving Gd to Super-Kamiokande to significantly enhance detection capability of neutrons from ν interactions

  J. F. Beacom and M. R. Vagins, Phys. Rev. Lett. 93 (2004) 17110

- Aiming for the **first observation of Diffuse Supernova Neutrino Backgrounds**

- Also aiming for:

  - Improving pointing accuracy for galactic supernova

  - Precursor of nearby supernova by Si-burning neutrinos

  - Reducing proton decay background

  - Neutrino/anti-neutrino discrimination (Long-baseline and atmospheric neutrinos)

  - Reactor neutrino measurements

- As the first step, loading 0.02% of $Gd_2(SO_4)_3$ in 2020

Meanwhile second loading completed (august 2022), taking data!

cross section
48.89kb
8MeV

From Talk by Y. Nakajima at Neutrino 2020 conference
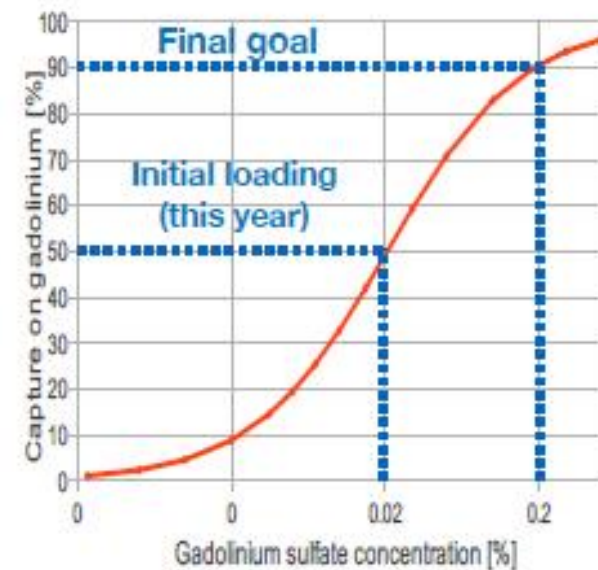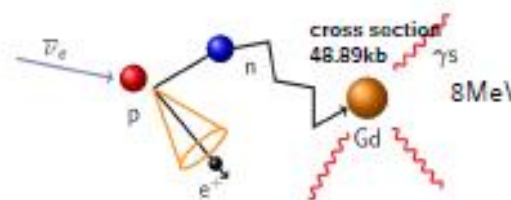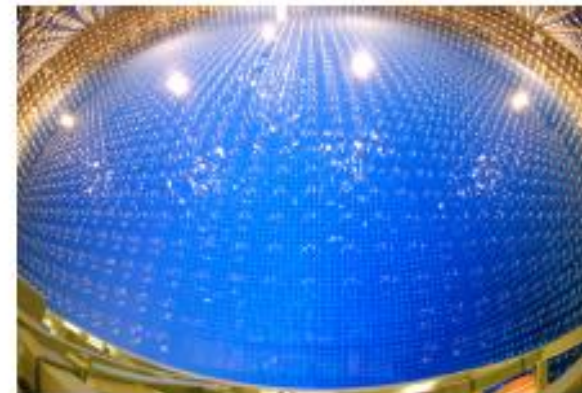
Geoneutrinos

Why are we interested in geoneutrinos?

Earth is unique among terrestrial planets:
- strongest magnetic field,
- highest surface heat flow,
- most intense tectonic activity,
- only one with continents composed of silicate crust

Understanding **the thermal**, geodynamical, and geological **evolution of** our planet is one of the most fundamental questions in Earth Sciences

Seismology gives precise information about density profile of the deep Earth , but it lacks direct information about the chemical composition and **radiogenic heat production.**
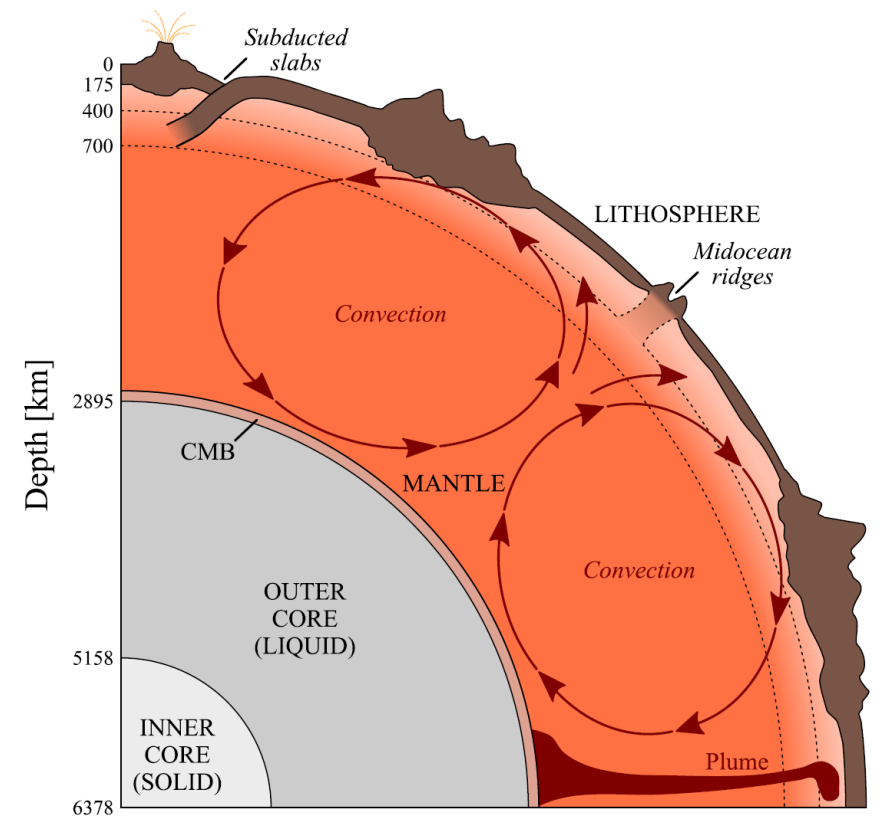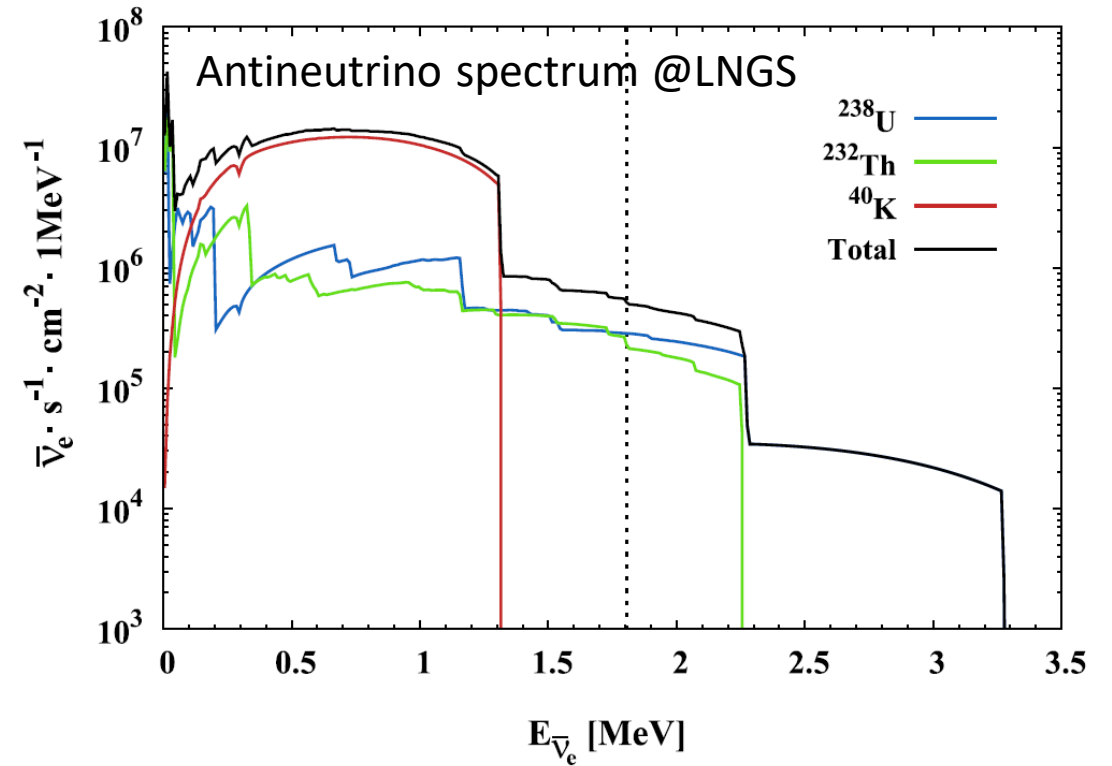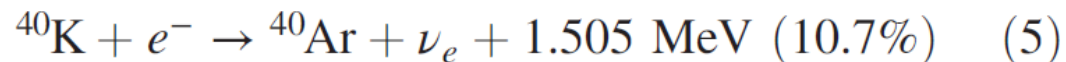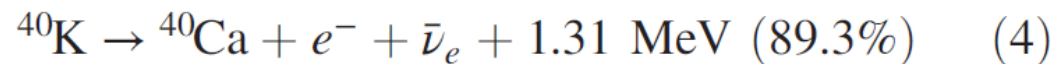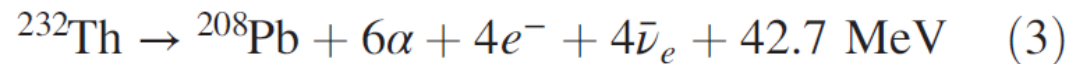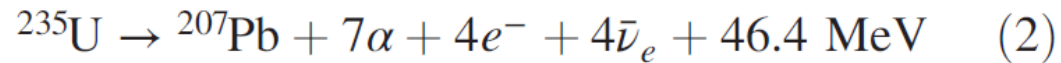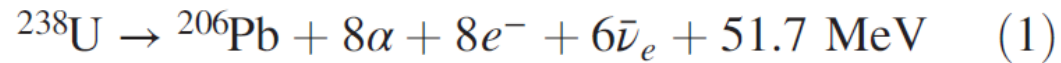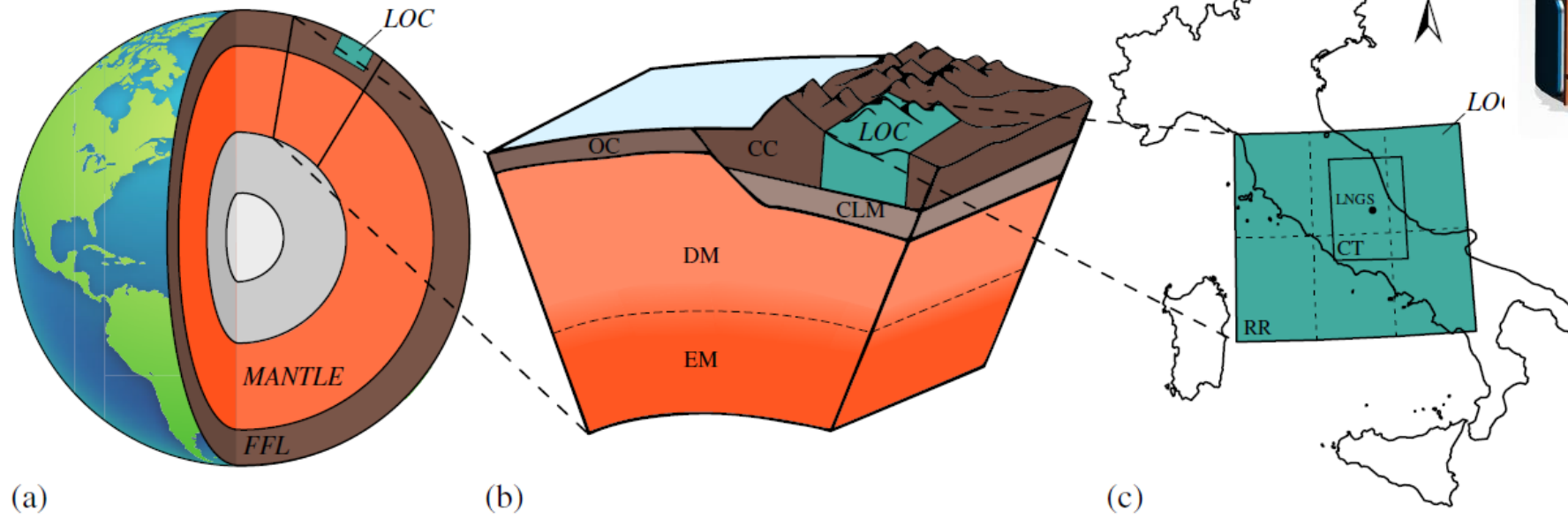
→ Geoneutrinos

FIG. 1. Schematic cross section of the Earth. The Earth has a concentrically layered structure with an equatorial radius of 6378 km. The metallic *core* includes an inner solid portion (1220 km radius) and an outer liquid portion which extends to a depth of 2895 km, where the core is isolated from the silicate *mantle* by the *core-mantle boundary* (CMB). Seismic tomography suggests a convection through the whole depth of the viscose mantle, that is driving the movement of the *lithospheric tectonic plates*. The lithosphere, subjected to brittle deformations, is composed of the *crust* and *continental lithospheric mantle*. The *mantle transition zone*, extending from a depth of 400 to 700 km, is affected by partial melting along the midoceanic ridges where the *oceanic crust* is formed. The *continental crust* is more complex and thicker than the oceanic crust.

HPEs (Heat Producing Elements) and relevant reactions:

$$^{238}\text{U} \rightarrow {}^{206}\text{Pb} + 8\alpha + 8e^- + 6\bar{\nu}_e + 51.7 \text{ MeV} \quad (1)$$

$$^{235}\text{U} \rightarrow {}^{207}\text{Pb} + 7\alpha + 4e^- + 4\bar{\nu}_e + 46.4 \text{ MeV} \quad (2)$$

$$^{232}\text{Th} \rightarrow {}^{208}\text{Pb} + 6\alpha + 4e^- + 4\bar{\nu}_e + 42.7 \text{ MeV} \quad (3)$$

$$^{40}\text{K} \rightarrow {}^{40}\text{Ca} + e^- + \bar{\nu}_e + 1.31 \text{ MeV} \ (89.3\%) \quad (4)$$

$$^{40}\text{K} + e^- \rightarrow {}^{40}\text{Ar} + \nu_e + 1.505 \text{ MeV} \ (10.7\%) \quad (5)$$

- information about the composition of the Earth's interior
- insight into the radiogenic heat contribution to the measured Earth's surface heat flux
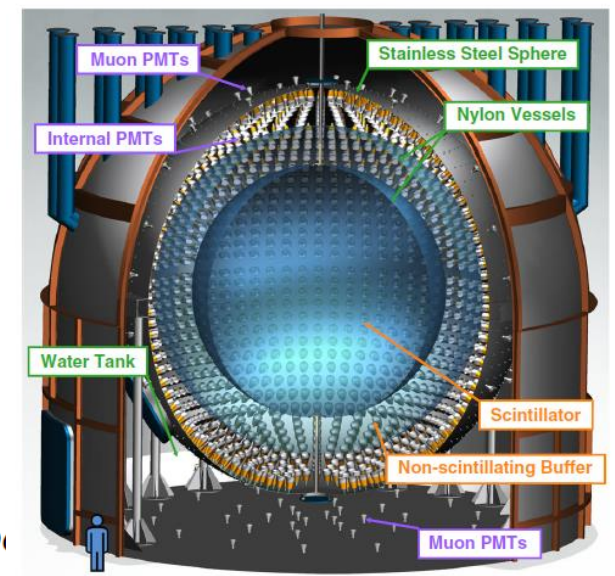
BOREXINO detector
@ LNGS

FIG. 15. (a) Schematic drawing of the Earth's structure showing the three units contributing to the expected geoneutrino signal at LNGS: (i) the *local crust* (LOC), (ii) the *far field lithosphere* (FFL), and (ii) the *mantle*. The inner and outer portions of the *core* (in grey) do not contribute to the geoneutrino signal. Not to scale. (b) Schematic section detailing the components of the BSE. The *lithosphere* includes the LOC and the FFL. The latter comprises the rest of the *continental crust* (CC), the *oceanic crust* (OC), and the *continental lithospheric mantle* (CLM). In the mantle, two portions can be distinguished: a lower *enriched mantle* (EM) and an upper *depleted mantle* (DM). Not to scale. (c) Simplified map of the LOC. The *central tile* (CT) of the $2° \times 2°$ centered at LNGS is modeled separately from the remaining six tiles which represent the *rest of the region* (RR).

Result from BOREXINO (2020)

based on the Borexino data acquired during 3262.74 days (2007 to 2019)

154 „golden" candidates
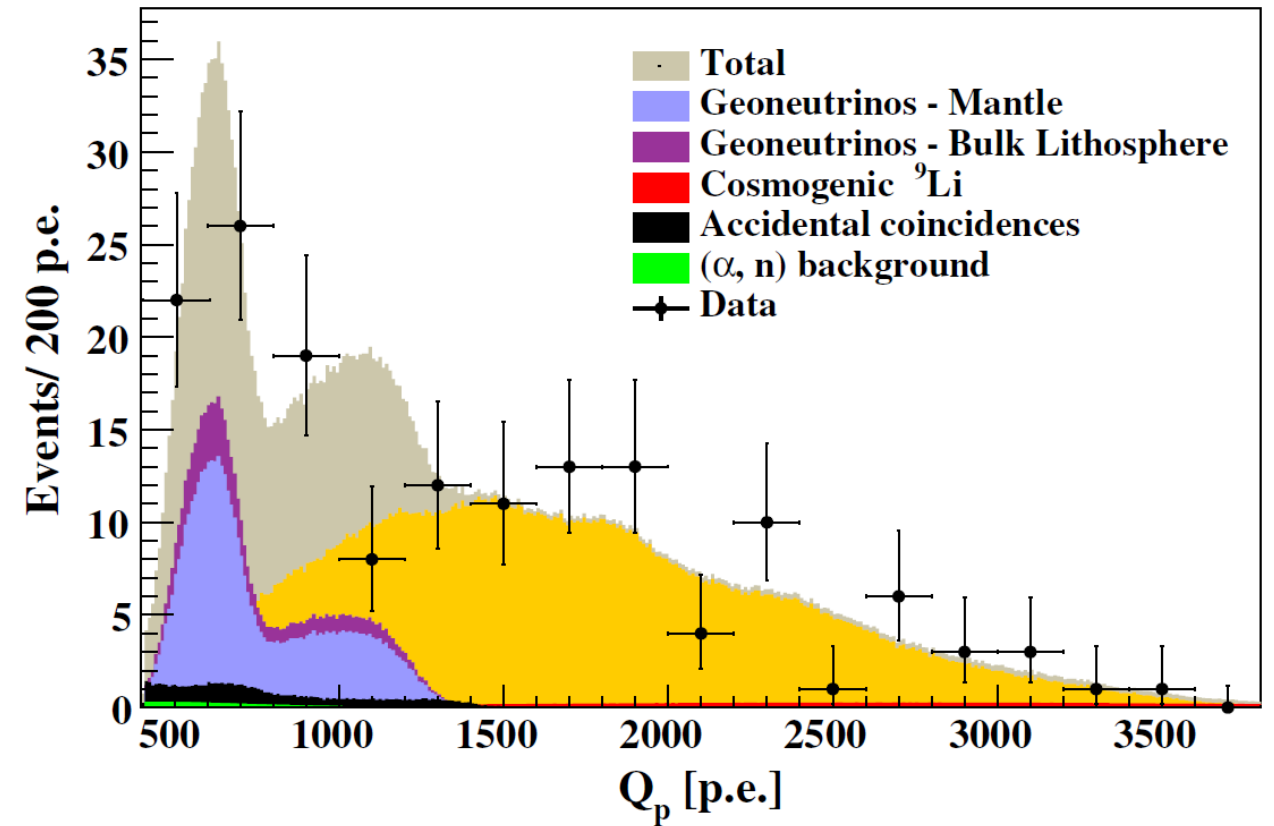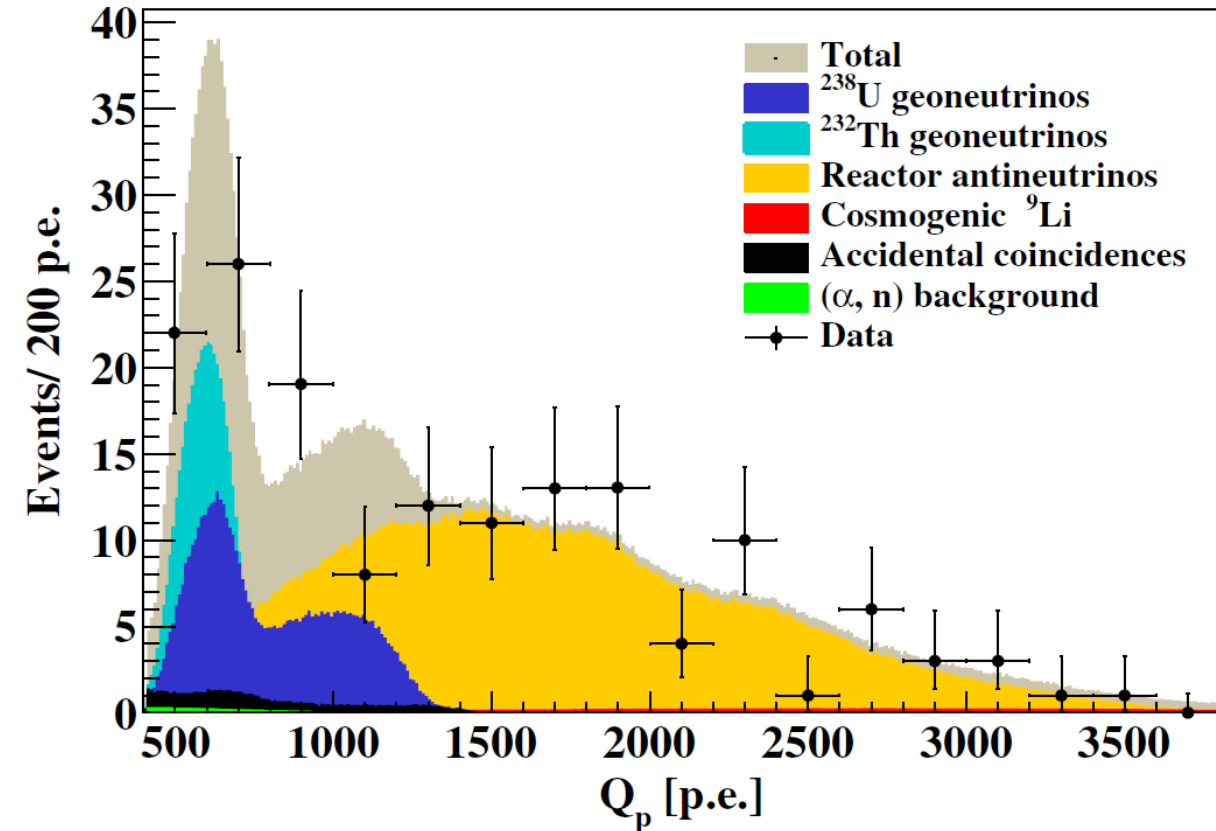
Borexino estimates the total radiogenic heat of the Earth $38.2^{+13.6}_{-12.7}$ TW